SEGMENTATION OF OCT SKIN IMAGES BY CLASSIFICATION OF SPECKLE STATISTICAL PARAMETERS

Mcheik Ali, Batatia Hadj

University of Toulouse, 2 rue Camichel BP 7122, 31071 Toulouse(France)

ABSTRACT

This paper deals with segmentation of dermatological OCT images. Classic image segmentation techniques fail to produce accurate results due to the wide presence of speckle. We propose using speckle as source of information in the segmentation process. Different statistical models are analyzed in terms of their ability to differentiate skin layers. The local speckle parameters are used as a features-vector to classify, in a supervised way, different regions. Experimental results are presented using a corpus of twenty three real images delineated by experts. These confirm the potential of the method to generate useful data for robust segmentation.

Index Terms— OCT, segmentation, speckle modeling, tissue characterization

1. INTRODUCTION

Human skin is a complex biological tissue consisting of stratified layers: epidermis (0.15 mm), dermis (1.2 to 1.8 mm) and hypodermis (1.2 mm). Its thickness varies with sex, age and region of the body. The diagnosis and treatment of skin pathologies are largely based on visual examination by dermatologists. Such examinations require a great experience due to the difficult interpretation of skin ambiguous states. Optical coherence tomography (OCT)[1] images allow the visualization of skin superficial structures, especially the stratum corneum and the junction between the dermis and the epidermis. However, the detailed examination of the images is strongly disturbed by the presence of speckle. This phenomenon reduces contrast and makes difficult the interpretation. It creates inter and intra experts variability when identifying the borders between the skin layers. Hence, the speckle is often regarded as a noise in OCT, and few denoising methods have been proposed [2, 3]. However, speckle is an important source of information to characterizing tissues. In [4], Hilman established that speckle contrast ratio in OCT depends on the local density of diffrators. In [5, 6], authors propose to analyze speckle texture and use it to distinguish different types of tissue. Notwithstanding, the segmentation of OCT images has received little interest in the literature. In this paper, we propose a classification method to segment skin layers in such images based exclusively on speckle information. Statistical models are fitted to the speckle by estimating their parameters. The derived parameters are analyzed in term of their ability to characterize skin layers. The parameters of the best model are used as the parameter vector to classify layers. The remainder of this paper is organized as follows. Section 2 presents the statistical models and the estimation of their parameters. Section 3 analyzes the parameters of these models in order to characterize skin layers. Section 4 presents the classification based segmentation. Finally, in section 5, we draw some conclusions and sketch research perspectives.

2. SPECKLE MODELING

In the literature, several statistical models have been applied to describe the distribution of speckle in various modalities of images [7, 8, 9]. In this work, we propose to use speckle statistics as information to segment OCT images. Our approach consists of fitting a statistical model to the speckle. The parameters are used as local features to classify skin layers. Four distributions are investigated, namely Rayleigh, Lognormal, Nakagami, and generalized Gamma. Their parameters are estimated using the method of moments. This section presents these models and their parameters.

Rayleigh distribution : This model was first introduced in a study dealing with speckle in laser imaging. It supposes a fully developed speckle, and derives from the central limit theorem. The backscattered signal can be modeled as a phasor sum of the returns from several scatters within the resolution cell of the system. The Rayleigh probability density function (pdf in the sequel) is given by:

$$p_R(q,\sigma) = \frac{q}{\sigma^2}\exp^{-\frac{q^2}{2\sigma^2}};\ \ q \geq 0;\ \sigma > 0 \qquad (1)$$

where σ is the scale parameter, and q the pixel intensity at (x,y). If nXm is the number of pixels, the estimation of σ by the methods of moments is given by:

$$\hat{\sigma} = \sqrt{\frac{2}{\pi}}\frac{\sum_1^n \sum_1^m q}{nm}. \qquad (2)$$

Lognormal distribution : The lognormal distribution has two parameters μ and σ. Its pdf is given by:

$$p_L(q,\mu,\sigma) = \frac{1}{\sigma q\sqrt{2\pi}} \exp^{-\frac{1}{2}\frac{(\log q-\mu)^2}{2\sigma^2}} \quad (3)$$

The parameters can be estimated based on the first two moments $m_1 = \sum_{i=1}^{n} \frac{x_i}{n}$ and $m_2 = \sum_{i=1}^{n} \frac{x_i^2}{n}$:

$$\begin{cases} \hat{\sigma} = \sqrt{\log \frac{m_2}{m_1^2}} \\ \hat{\mu} = 2\log(m_1) - \frac{1}{2}\log(m_2) \end{cases} \quad (4)$$

Nakagami distribution : The Nakagami distribution aims at modeling the dispersion of several backscattered clusters of waves added incoherently. We can show that the Rayleigh distribution is a particular case of Nakagami. It is also an approximation of Rice distribution. The signal to noise ratio of the Nakagami distribution can take any positive value. Its pdf is given by:

$$p_N(q,\mu,L) = \frac{2}{\mu}\frac{\sqrt{L}}{\Gamma(L)}\left(\frac{q\sqrt{L}}{\mu}\right)^{2L-1} \exp^{-\left(\frac{q\sqrt{L}}{\mu}\right)^2} \quad (5)$$

where L is the shape parameter and μ the scale parameter, with $q \geq 0$. As this function has two parameters, moments of order 1 and 2 need to be evaluated:

$$\begin{cases} \hat{L} = \frac{1}{8}\frac{1}{\frac{\sqrt{m_2}}{m_1}-1} \\ \hat{\mu} = \sqrt{m_2} \end{cases} \quad (6)$$

Generalized gamma distribution (GG3): The GG3 function is a highly flexible three parameter distribution. It has been shown to generalize several other distributions such as Weibull and Lognormal. The pdf of this distribution may be written as:

$$P_G(q,\gamma,\rho,\beta) = \begin{cases} \frac{\beta^{-\rho}}{\Gamma(\rho)}(q-\gamma)^{\rho-1}\exp^{\frac{-(q-\gamma)}{\beta}} \\ 0,\ if\ \gamma > q, \rho < 0 \end{cases} \quad (7)$$

where γ is the threshold or location parameter, ρ the shape parameter and β the scale parameter. The mean, variance, mode, third standard moment and the fourth standard moment of the random sample $I = \{I(x,y)\}; x = 1..n; y = 1..m$, are:

$$E(I) = \gamma + \rho\beta;\ V(I) = \rho\beta^2;\ M_o(\mathrm{I}) = \gamma + \beta(\rho-1) \quad (8)$$

$$\alpha_3 = \frac{2}{\sqrt{\rho}};\ \alpha_4 = 3 + \frac{3}{2}\alpha_3^2. \quad (9)$$

We estimate the three parameters (γ,ρ,β) with the classical method of moments, by equating the first three sample moments to corresponding distribution moments. Let I_{low} be the lowest sample observation. Approximating $\gamma = I_{low}$, we can show that the two other parameters can be estimated as follows:

$$\hat{\beta} = \frac{\sigma_e}{\overline{I} - I_{low}}, \quad \hat{\rho} = \frac{\overline{I}-I_{low}}{\beta} = \frac{(\overline{I}-I_{low})^2}{\sigma_e} \quad (10)$$

3. SKIN LAYER CHARACTERIZATION

Goodness of fit : In order to assess the ability of the four models to characterize skin layers, we conducted an empirical study of their parameters. Twenty three skin OCT images annotated by five expert dermatologists have been analyzed. Each expert drew three curves separating the skin surface, the stratum corneum, and the frontier between the epidermis and the dermis (Fig. 1). The parameters of each distribution were estimated for the stratum corneum and the (remainder of) epidermis. Figure 2 presents the theoretical and the estimated distributions for the two layers. We evaluated the goodness of fit of the four models using the Kolmogorov-Smirnov (KS) quantitative indicator [10] (Fig. 3). We concluded empirically that the GG3 model represents best the distribution of speckle OCT skin images. However, Nakagami presents acceptable scores as opposed to Lognormal and Rayleigh. We only retained the two first distributions for further analysis.

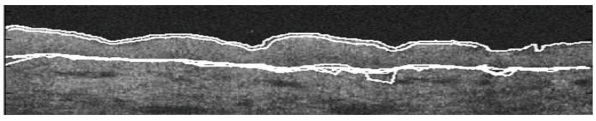

Fig. 1. Optical coherence tomography images with manual expert delineations.

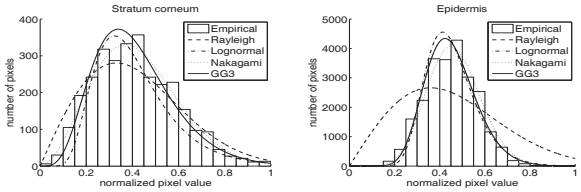

(a) (b)

Fig. 2. Fitting distributions to empirical data. (a) stratum corneum. (b) epidermis.

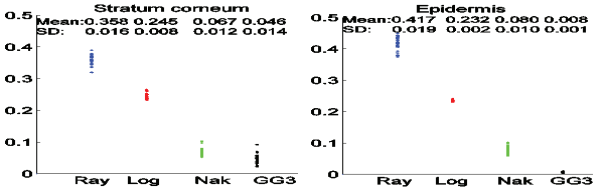

(a) (b)

Fig. 3. KS goodness of fit to 23 images data. (a) stratum corneum. (b) epidermis.

Layer separability : We then evaluated the ability of the

	$Nakagami$		$GG3$	
	$\hat{SC}$	$\hat{EP}$	$\hat{SC}$	$\hat{EP}$
SC	526	74	592	8
EP	71	529	17	583
$Accuracy\%$	87	88	98	97
$Error\ rate$	0.1208		0.0208	

Table 1. Confusion matrices of two distributions. SC: stratum corneum. EP: rest of epidermis.

	$Nakagami$			
	$\mu_{Nakagami}$		$\mathcal{L}_{Nakagami}$	
	$\hat{SC}$	$\hat{EP}$	$\hat{SC}$	$\hat{EP}$
SC	548	52	414	186
EP	78	522	133	467
$Accuracy\%$	91	87	69	77
$Error\ rate$	0.1083		0.2633	

Table 2. Confusion matrices of parameters of Nakagami. SC: stratum corneum. EP: rest of epidermis.

GG3 and Nakagami parameters to discriminate the two layers. For this purpose, we adopted a support vector machine classification. The parameters estimated from every layer (as outlined by experts) in each image were used as input vector to the classifier whose output were the two layers. Eighty percent (80%) of the images were used to train the classifier. The remaining 20% allowed testing the precision of the classification. This process has been repeated 100 times to study the variability of the classification against the training set. For each classifier, we measured the precision using the confusion matrix. Table 1 shows the averaged matrix over the 100 experiments. It shows the excellent score of the GG3 to differentiate, globally, between stratum corneum and epidermis.

Individual parameters : This result involves the use of the whole vector of parameters for each distribution. In order to check wether a subset of these parameters explains this results, we analyzed individually the parameters in the same manner. Tables 2 and 3 show the averaged confusion matrix for each parameter for Nakagami and GG3, respectively. The results indicate that μ and β, respectively for Nakagami and GG3, are the parameters that capture better the spatial information of the speckle in both layers. Consequently, we retained only these two parameters for the segmentation method (see sec. 4).

4. SKIN LAYER SEGMENTATION

Based on the above result, we designed a segmentation method in order to separate skin layers based on their speckle distributions. For this purpose, we adapted our estimator to

	$GG3$					
	γ_{GG3}		ρ_{GG3}		β_{GG3}	
	$\hat{SC}$	$\hat{EP}$	$\hat{SC}$	$\hat{EP}$	$\hat{SC}$	$\hat{EP}$
SC	405	195	542	58	590	10
EP	170	430	35	565	20	580
$Accuracy\%$	67	71	90	94	98	96
$Error\ rate$	0.304		0.077		0.025	

Table 3. Confusion matrices of parameters of GG3. SC: stratum corneum. EP: rest of epidermis.

estimate parameters in the vicinity of the pixel. Only parameters μ and β, respectively for Nakagami and GG3, were considered. One speckle parameter has therefore been associated with each pixel, for each distribution. The underlying idea is that local parameters of the same layer have a statistical coherence that distinguish them from those of other layers. This idea has been confirmed by applying a simple Canny filter on the map of parameters (Fig. 4.a). Based on this principle, we designed a pixel classification method similar to that of the layers (as seen above). A support vector machine classifier was established, where the input features-vector was the local parameter of the speckle in the neighborhood of the pixel, and the output is the layer to which belongs the pixel.

Stability of the estimator : Before using local parameters, we evaluated the stability of our estimators against the amount of data used. Data samples of various sizes (from 0 to 200) were simulated using the two distributions with different parameters. The evaluation method consisted of estimating the parameters that best fit the models to the simulated data set. Parameters estimated, in 7x7 neighborhood, were compared to theoretical ones in terms of KS test. Only results for GG3 are shown in figure (4.b). The scores are below the KS significance scale [10] for all sample sizes. This means that our estimators are stable and can be used with small samples around a pixel.

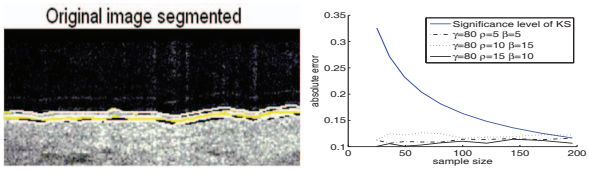

(a) (b)

Fig. 4. (a) Results of Canny filter on stratum parameters map, β: black, μ: white, expert: yellow. (b) Stability of the GG3 parameters estimator.

Classification : For each model (Nakagami and GG3), we trained an SVM classifier with 20% pixel selected randomly in each layer from all (23) images. Classifiers were tested on

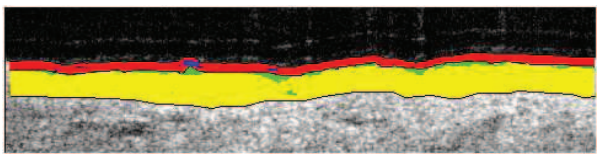

Fig. 5. Layer segmentation by classification of speckle parameters. Red: true positive stratum, blue: false positive epidermis, Yellow: true positive epidermis, Green: false positive stratum.

the 80 % remaining pixels. As mentioned higher, the input of the classifier were the statistical parameters of each pixel, and the output the corresponding layer as delineated by experts. As an illustration, an image classified with GG3 is shown in figure 5. The reader can note the visual predominance of true positives for the two layers. This is especially important for the stratum layer given its very small thickness (3 to 5 pixels). Pixels found as belonging to epidermis, where experts classified them as stratum, are mainly along the border between the two layers. This can be explained by the effect of estimating parameters from populations made necessarily of pixels from different layers. It can also follow from experts imprecision. In order to assess the variability of the classifier against the training set, we repeated the previous experimentation 100 times. The variation of the global producer precision is shown in figure 6, respectively for Nakagami and GG3. The results show that GG3 has higher potential to segment layers. We have indeed obtained for this model a precision of 80% for the stratum and 98% for the epidermis.

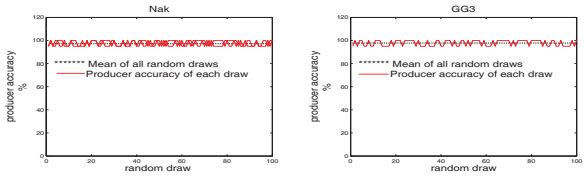

(a) (b)

Fig. 6. Precision of the classifiers against the training sets.

5. CONCLUSION

We presented in this paper a study of skin tissue characterization in OCT images based on the statistical distribution of speckle. Four statistical models have been fit to the images by estimating their parameters using the method of moments. A corpus of twenty three skin images have been used in the study. The parameters of GG3 and Nakagami have been shown to represent correctly skin layers. In addition, individual parameters of these distributions have been analyzed for the characterization of the layers, using SVM classifiers. One parameter of each distribution has been found to capture the spatial statistical configuration of the data. Based on this result, we designed a segmentation method based on the SVM classification of the local parameters of the speckle. This has been applied to the separation of the stratum corneum from the rest of the epidermis. The results show excellent precision with the GG3. Moreover, we have noticed little variability of the classification precision against training sets. We are currently investigating an unsupervised classification method to segment layers and melanoma in skin tissues.

6. REFERENCES

[1] A.F. Fercher, W. Drexler, C.K. Hitzenberger, and T. LAsser, "Optical coherence tomography-principles and applications," *Institut of Physics Publishing, Rep. Prog. Phys.66 239-303*, 2003.

[2] M. Bashkansky and J. Reinjtes, "Statistics and reduction of speckle in optical coherence tomography," *Optics Letters*, vol. 25, pp. 545–547, 2000.

[3] N.Iftimia, B.Bouma, and G.J.Tearney, "Speckle reduction in optical coherence tomography by encoded angular compounding," *Journal of Biomed.opt*, vol. 8, pp. 260–263, 2003.

[4] T.R. Hillman, S.G. Adie, V. Seemann, and J.J. Armstrong, "Correlation of statistic speckle with sample properties in optical coherence tomography," *OPTICS LETTERS*, vol. 31, january 2006.

[5] K.W. Gossage, T.S. Tkaczyk, J.J. Rodriguez, and J.K. Barton, "Texture analysis of optical coherence tomography images: feasibility for tissue classification," *J.Biomed.Opt*, vol. 8, pp. 570, 2003.

[6] K.W. Gossage et al, "Texture analysis of speckle in optical coherence tomography images of tissue phantoms," *Physics in Medicine And Biology*, vol. 51, pp. 1563–1575, 2006.

[7] J.M. Schmitt, "Optical coherence tomography(oct)," *a review, IEEE Journal of Selected Topics in Quantum Electronics*, vol. 5, pp. 1205–1215, july 1999.

[8] J.W. Goodman, "Speckle phenomena in optics:theory and applications," *Englewood. Roberts and company, Etats-Unis*, 2007.

[9] B.I. Raju and M.A. Srinivasan, "Statistics of envelope of high-frequency ultrsonic backscatter from in vivo," *IEEE Transaction on Ultrasonics, Ferroelectrics and frequency Control*, vol. 49, pp. 871–882, 2002.

[10] W. J Conover, "Practical nonparametric statistics," *New York ; Chichester:Wiley*, 1980.